

Silent *IL2RG* Gene Editing in Human Pluripotent Stem Cells

Li B Li¹, Chao Ma^{2,3}, Geneve Awong^{4,5,6,9}, Marion Kennedy^{4,5,6}, German Gornalusse¹, Gordon Keller^{4,5,6}, Dan S Kaufman^{3,7} and David W Russell^{1,8}

¹Department of Medicine, University of Washington, Seattle, Washington, USA; ²College of Veterinary Medicine, University of Minnesota, Minneapolis, Minnesota, USA; ³Department of Medicine, University of Minnesota, Minneapolis, Minnesota, USA; ⁴McEwen Centre for Regenerative Medicine, University Health Network, Toronto, Ontario, Canada; ⁵Princess Margaret Cancer Centre, University Health Network, Toronto, Ontario, Canada; ⁶Department of Medical Biophysics, University of Toronto, Toronto, Ontario, Canada; ⁷Stem Cell Institute, University of Minnesota, Minneapolis, Minnesota, USA; ⁸Department of Biochemistry, University of Washington, Seattle, Washington, USA; ⁹Current address: Sunnybrook Research Institute, Toronto, Ontario, Canada.

Many applications of pluripotent stem cells (PSCs) require efficient editing of silent chromosomal genes. Here, we show that a major limitation in isolating edited clones is silencing of the selectable marker cassette after homologous recombination and that this can be overcome by using a ubiquitous chromatin opening element (UCOE) promoter-driven transgene. We use this strategy to edit the silent *IL2RG* locus in human PSCs with a recombinant adeno-associated virus (rAAV)-targeting vector in the absence of potentially genotoxic, site-specific nucleases and show that *IL2RG* is required for natural killer and T-cell differentiation of human PSCs. Insertion of an active UCOE promoter into a silent locus altered the histone modification and cytosine methylation pattern of surrounding chromatin, but these changes resolved when the UCOE promoter was removed. This same approach could be used to correct *IL2RG* mutations in X-linked severe combined immunodeficiency patient-derived induced PSCs (iPSCs), to prevent graft versus host disease in regenerative medicine applications, or to edit other silent genes.

Received 20 May 2015; accepted 30 September 2015; advance online publication 3 November 2015. doi:10.1038/mt.2015.190

INTRODUCTION

Many applications require that silent genes be edited. This is especially true for pluripotent stem cells (PSCs), which may not express the tissue-specific genes responsible for diseases. For example, in one common paradigm for regenerative medicine, PSCs reprogrammed from a patient's cells would be propagated as undifferentiated cells, the disease-causing mutations present in silent genes such as β -globin (*HBB*) or interleukin 2 receptor gamma (*IL2RG*) would be corrected by gene editing, and the corrected cells would then be differentiated into a therapeutic cell product. The creation of isogenic PSC-based cellular disease models requires the same types of genetic manipulations, as does the engineering of lineage specification genes.

Transcription has long been known to increase homologous recombination¹ and gene targeting by transfection-based methods.²

One way to overcome this limitation is the introduction of sequence-specific double-strand breaks (DSBs) by engineered nucleases in order to enhance silent gene targeting. For example, zinc finger nucleases (ZFNs) and transcription activator-like effector nucleases (TALENs) have been used to isolate human PSC clones edited at *PITX3* (ref. 3), *HBB*,^{4,5} and *IL2RG*.^{6,7} However, it seems likely that these site-specific DSBs did not completely eliminate the bias against editing silent loci, since the targeting frequencies were lower than those of expressed genes in these same cell types.^{3,4} The use of engineered nucleases may also lead to a variety of genotoxic effects, including unwanted sequence changes at on- and off-target sites,^{6,8} which could be a disadvantage in some settings.

Alternatively, the lower targeting frequencies observed at silent loci could be due to inadequate expression of the selectable marker gene after it integrates, rather than a decrease in homologous recombination. This appears to have occurred when a hygromycin resistance cassette was inserted into the *HBB* gene in human PSCs, since the gene-edited cells lost hygromycin resistance over time.⁴ This example highlights the poorly understood epigenetic changes that presumably occur during silent gene editing, which include potential alterations induced by the recombination and repair enzymes acting on the locus, the effects of introducing an expressed selectable marker into silent chromatin, and in many cases, the subsequent removal of that same expressed marker after isolating an edited clone. In general, the epigenetic consequences of gene editing remain an important but largely unexplored area of research. Two notable exceptions are studies showing that gene expression and DNA methylation can be altered in mice derived from embryonic stem cells (ESCs) with gene-targeted, imprinted loci,^{9,10} and a recent report showing that DNA methylation can be rendered unstable at a gene-targeted locus in Arabidopsis.¹¹ The epigenetic effects of gene editing in human cells have not yet been described.

In this study, we use recombinant adeno-associated virus (rAAV) vectors to edit silent genes in human PSCs. rAAV vectors deliver single-stranded linear DNA genomes that efficiently recombine with homologous chromosomal sequences in human cells,¹² including PSCs.^{13–15} Under optimal conditions, between 0.1 and 1% of normal human cells exposed to rAAV targeting

vectors undergo high fidelity gene editing at expressed target loci,^{12,16} without a requirement for site-specific nucleases. To date, rAAV vectors have not been used to edit silent genes in PSCs, although rAAV-mediated editing of silent genes has been demonstrated at lower frequencies in hepatocytes and fibroblasts.¹⁷⁻¹⁹ Here, we evaluate different selectable marker cassettes to develop a robust, silent gene-editing method for human PSCs that does not require a site-specific nuclease, we examine the epigenetic consequences of targeting silent loci, and we determine the developmental effects of *IL2RG* gene editing.

RESULTS

Transgene promoter type determines targeted clone survival

In order to optimize vector designs, we developed an assay to detect gene-editing events at a nontranscribed locus, in which only gene-targeted cells survive selection (Figure 1a). The assay uses induced pluripotent stem cells (iPSCs) containing a silenced *Neo* gene that can be activated by upstream promoter insertion. We first infected human mesenchymal stem/stromal cells (MSCs) with a rAAV knock-in vector designed to insert a *Neo* gene at

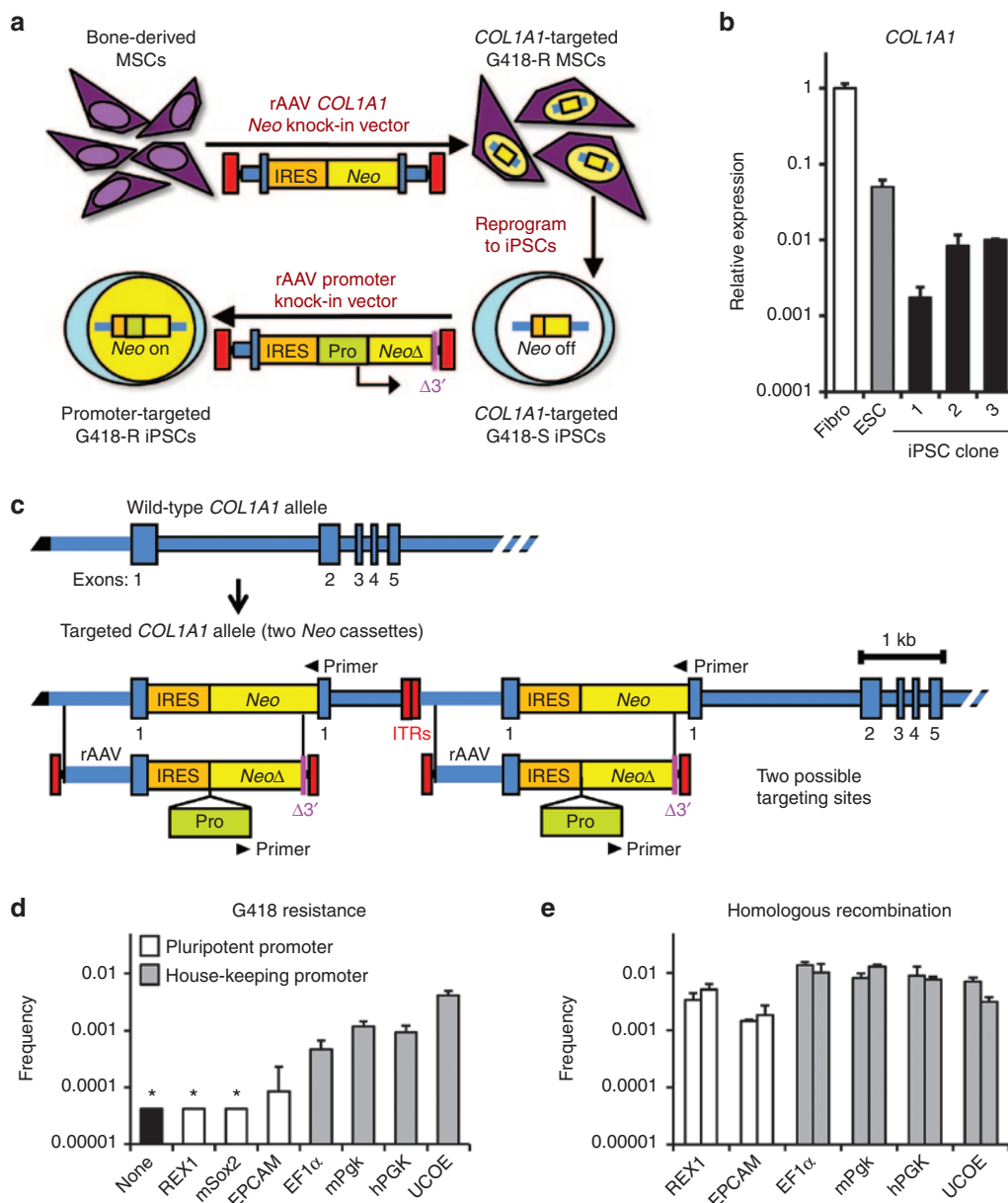


Figure 1 Targeting a silent *COL1A1*-IRES-*Neo* cassette in human iPSCs. **(a)** Diagram of experimental design. **(b)** RT-qPCR of *COL1A1* expression in undifferentiated iPSC clones containing *COL1A1*-IRES-*Neo* knock-ins. Fibro, human fibroblasts; ESC, undifferentiated H1 cells. **(c)** Structures of wild-type and IRES-*Neo* targeted *COL1A1* alleles in iPSC clone 1 with rAAV promoter knock-in vector overlap indicated. The targeted *COL1A1* locus contains two identical IRES-*Neo* cassettes, each of which can be targeted by rAAVs. Black triangles, primer-binding sites used for qPCR measurements of homologous recombination frequencies. **(d)** G418 resistance frequencies of iPSC clone 1 infected with promoter knock-in rAAVs. *less than 4×10^{-5} . **(e)** Homologous recombination frequencies measured by qPCR with primers shown in **c**. Each infected cell population was analyzed with two primer pairs.

the endogenous *COL1A1* locus encoding type I collagen, which is highly expressed in MSCs. A polyclonal population of G418-resistant MSCs was then converted to iPSCs by expressing *OCT4*, *SOX2*, *NANOG*, and *LIN28* transgenes.²⁰ Three of these iPSC clones were analyzed further, and clone 1 had the lowest level of *COL1A1* expression after reprogramming (Figure 1b). Southern blot analysis showed that this clone also had a duplication of the *Neo* transgene (Supplementary Figure S1c), which happens in a small percentage of targeted clones when vector genomes form dimers before recombination.¹⁶ Although this complicated our analysis, we confirmed that clone 1 was completely sensitive to G418 (Supplementary Figure S1a), so both *Neo* transgenes had been silenced and could therefore be activated by promoter insertion. The residual *COL1A1* transcription detected in clone 1 cells may have been derived from the subpopulation of differentiating cells present in PSC cultures, which do not contribute to the PSC clones isolated by selection.

A series of gene editing vectors were designed to insert different promoters upstream of either silenced *Neo* transgene cassette, each of which contained a truncated *Neo* gene fragment in the right homology arm so that random integration could not confer G418-resistance, and only gene-edited clones would survive selection (Figure 1c). Two types of promoters were incorporated into the rAAV gene-editing vectors: developmentally regulated promoters that are expressed in human PSCs (REX1, murine Sox2, and EPCAM), and ubiquitously expressed promoters (EF1 α , murine Pkg, human PGK, and ubiquitous chromatin opening element [UCOE]). When clone 1 PSCs with silenced *Neo* genes were infected with each of these vectors at the same multiplicity of infection, there were dramatic differences in the number of G418-resistant colonies obtained (Figure 1d), with the UCOE promoter producing the highest number. Southern blots showed that the G418-resistant colonies had been targeted at one of the two silent *Neo* gene targets (examples in Supplementary Figure S1c).

For a subset of vectors, gene-editing frequencies were also measured in unselected cells directly by qPCR, using one primer within the inserted promoter and one in chromosomal DNA outside of the homology arm (Figure 1e and Supplementary Figure S1b). This showed that despite a more than 100-fold difference in their ability to produce G418-resistant colonies, the REX1, EPCAM, EF1 α , mPkg, hPGK, and UCOE promoter vectors all produced homologous recombinants at similar frequencies. Thus, rAAV vectors can edit a silent *COL1A1* gene in human PSCs regardless of the transgene promoter they contain, but transgene selection requires a promoter that can drive expression at a silent locus. In the case of the UCOE promoter, the G418-resistance and homologous recombination frequencies were very similar, suggesting that almost every recombination event produced a G418-resistant cell. One potential drawback of the UCOE promoter is its relatively large size. Unfortunately, smaller promoter fragments did not produce as many G418-resistant colonies (Supplementary Figure S1d). These experiments demonstrate that the 1.2 kb UCOE promoter can be used to select for PSCs that undergo silent gene editing.

Editing of the silent *IL2RG* gene

IL2RG encodes a common subunit for several cytokine receptors expressed in hematopoietic cells and is mutated in individuals

with X-linked severe combined immunodeficiency (X-SCID). *IL2RG* is not expressed at a detectable level in human PSCs as measured by global expression arrays and RT-qPCR (data not shown and Figure 2b), is present as a single copy in male cells, and represents a promising target for developing PSC-based therapies. We therefore tested if a rAAV editing vector could be used to insert a UCOE-*Neo*-pA (UNA) cassette into exon 2 of *IL2RG* (Figure 2a). H1 human ESCs (a male cell line) were infected with vector AAV-*IL2RG*e2UNA and 3 of 18 G418-resistant colonies screened by PCR were targeted at the *IL2RG* gene (Supplementary Figure S2a). This represented 17% of G418-resistant colonies and 0.14% of the unselected cell population, which was similar to what we observed when targeting the *COL1A1* locus, confirming that the UCOE promoter could be used to select for PSC clones with edited *IL2RG* genes.

Many gene-editing applications also require the removal of the selectable marker cassette, so that only a linked, subtle editing

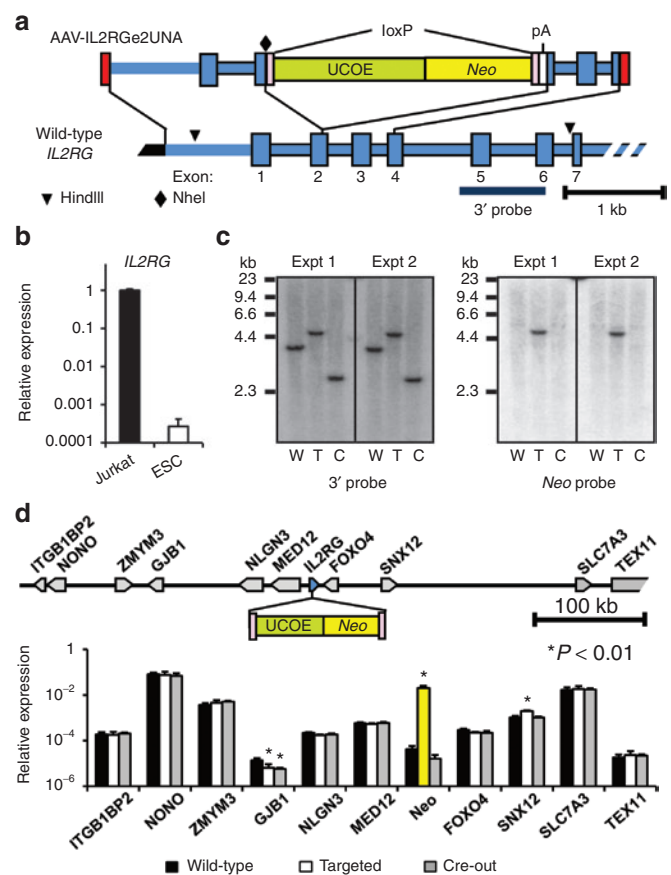


Figure 2 Targeting a silent *IL2RG* gene in human ESCs. **(a)** Structure of the *IL2RG* locus and rAAV targeting vector, with the locations of restriction enzyme sites and probe used in **c**. **(b)** RT-qPCR of *IL2RG* expression in undifferentiated ESCs. **(c)** Southern blot performed on age-matched wild-type (W), targeted (T), and Cre-out (C) clones, digested with HindIII and NheI and probed with a 3' chromosomal fragment outside the homology arm, which produces fragments of 3.8, 4.7, and 2.6 kb in wild-type, targeted, and Cre-out clones, respectively. The same blot was stripped and re-probed with a *Neo* fragment. **(d)** RT-qPCR of gene expression of *IL2RG*'s genomic neighbors and *Neo* in age-matched wild-type, targeted, and Cre-out clones. Relative expression signals were normalized to *GAPDH* and plotted as 2^{-(CT of gene - CT of GAPDH)}. Statistical significance was calculated by comparing to wild-type cells. **P* < 0.01.

change remains. Vector AAV-IL2RGe2UNA was designed so that Cre-mediated recombination would remove the floxed *Neo* cassette and leave behind a polyadenylation signal and three stop codons to inactivate *IL2RG*. We infected two different *IL2RG*-targeted clones with a nonintegrating foamy virus vector that transiently expressed Cre,²¹ and efficiently removed the *Neo* transgene cassette from 6–28% of cells (Supplementary Figure S2b). Southern blots confirmed the structures of the targeted and Cre-out alleles, as well as the lack of random integrants in targeted clones (Figure 2c).

Ideally, the editing of a silent locus would not affect the expression of other genes, so we analyzed neighboring gene expression in 10 genes spanning a 700 kb window surrounding *IL2RG* (Figure 2d). One gene (*SNX12*) had slightly increased expression in targeted cells that still contained the UCOE-*Neo* cassette, reflecting a potential long distance effect of the UCOE promoter. A second gene (*GJB1*) had statistically significant changes in RT-qPCR measurements, but all values were below those of the *Neo* signal from control cells lacking a *Neo* gene, suggesting a lack of expression. The eight other genes had no significant changes in expression, including the three genes located closest to *IL2RG* (*NLGN3*, *MED12*, and *FOXO4*), indicating that *IL2RG* gene targeting and subsequent Cre-out had minimal impact on neighboring gene expression.

Epigenetic consequences of gene editing

Insertion of an active promoter could change the epigenetic status of the surrounding chromatin, as could the recombination and repair proteins that carry out homologous recombination, yet the epigenetic consequences of gene editing remain a largely unexplored area of research. One possible effect is removal of 5-methylcytosine (5mC) residues in DNA, in particular at CpG islands, which are typically methylated in silent loci.²² The wild-type *COL1A1* gene contains a CpG island that was duplicated in the PSC clone we used for promoter insertion studies (Figure 3a). When the locus is silent, these CpG islands are highly methylated, but after UCOE promoter insertion at either duplicated site, one of the islands became mostly unmethylated (Figure 3b). Although the bisulfite sequencing reaction does not distinguish between the two islands, these results are consistent with a localized region of hypomethylation at the CpG island nearest to the UCOE insertion site. Since this region is included within the 5' homology arm of the UCOE insertion vector, incorporation of the unmethylated vector genome could have led directly to the loss of 5mC residues. In support of this hypothesis, we confirmed that the packaged rAAV vector genome was unmethylated (Figure 3b), and we showed previously that the entire homology arm sequence extending to the terminal repeats are typically incorporated into a targeted locus.²³ Unfortunately, a similar analysis could not be performed at the *IL2RG* locus, which does not contain a CpG island within the homology region. We found no consistent difference in the methylation status of eight nonisland CpGs present in the *IL2RG* gene that were assayed in wild-type cells and knockout cells, suggesting that UCOE promoter insertion may not lead to demethylation of nonisland CpGs (Supplementary Figure S3).

Histone modifications can also vary depending on the transcriptional activity of a locus and other factors. Although many such modifications have been described, here we studied acetylation and

methylation at lysine 27 of histone H3 (H3K27Ac and H3K27Me3), which are associated with active and silent chromatin, respectively.^{24–26} In the case of *COL1A1*, the 1 kb region immediately surrounding the UCOE insertion site that includes the IRES element and *Neo* gene contained H3K27Me3 markers before UCOE insertion, indicative of silent chromatin (Figure 3c). After UCOE insertion, this pattern changed to one of active chromatin, with an increase in H3K27Ac levels that extended throughout the duplicated locus to sites 2.8 and 8.4 kb distal to the insertion site, as well as lower levels of H3K27Me3 in the more localized IRES and *Neo* regions. Interestingly, the change in H3K27Ac markers extended to regions outside of the homology arms, demonstrating that epigenetic changes had been propagated beyond the recombination site.

We studied the same histone markers at the *IL2RG* locus, only in this case, the analysis was more relevant because the target was single copy, the UCOE promoter was inserted at a wild-type gene that had not been previously targeted, and we could assay after both UCOE insertion and subsequent Cre-mediated UCOE removal. The wild-type locus had low levels of H3K27Ac and higher levels of H3K27Me3 throughout a 3.3 kb region surrounding the exon 2 insertion site, consistent with silent chromatin (Figure 3d). Insertion of the UCOE-*Neo* cassette activated this entire locus, including regions beyond the vector homology arms, as evidenced by increased H3K27Ac levels. However, unlike the *COL1A1* locus, we did not observe a corresponding reduction in H3K27Me3 throughout this region. Instead, the decrease in H3K27Me3 was only observed downstream of the UCOE-*Neo* cassette. The basis for this asymmetry is unclear and was not shared by *COL1A1*, which had decreased H3K27Me3 levels on both sides of the UCOE insertion site. Importantly, once the UCOE-*Neo* cassette was removed by Cre-mediated recombination, the epigenetic status of the entire locus reverted back to that of the wild-type locus.

IL2RG-knockout human ESCs model X-SCID *in vitro*

While *IL2RG* mutation correction could be used to treat X-SCID, inactivation of *IL2RG* by gene editing could also have applications in regenerative medicine. For example, when differentiating pluripotent cells into hematopoietic progeny to be used for transplantation, it may be desirable to prevent the formation of natural killer (NK) or T cells that could react against host cells in a form of graft versus host disease. Based on the phenotype of X-SCID patients,^{27,28} and the known roles of the cytokine receptors that include IL2RG subunits,²⁹ we predicted that *IL2RG* knockout stem cells should not produce NK or T cells *in vitro*.

We first differentiated wild-type and *IL2RG*-edited ESC lines into embryoid bodies (EBs) containing hematopoietic progenitors, which were then selectively differentiated into NK or T cells as described.^{30,31} After 8 days of NK differentiation, all the ESC lines produced similar numbers of cells expressing the CD56 NK marker, including CD2+ and CD7+ early lymphoid subsets (Figure 4a). In comparison, NK differentiation of CD34+ cells isolated from umbilical cord blood cells produced fewer CD56+ cells and lower expression levels of CD7. However, after 22 days of differentiation, the umbilical cord blood and wild-type EB cultures both contained nearly 80% CD56+ NK cells with substantial CD2+ and CD7+ subpopulations that were largely absent from

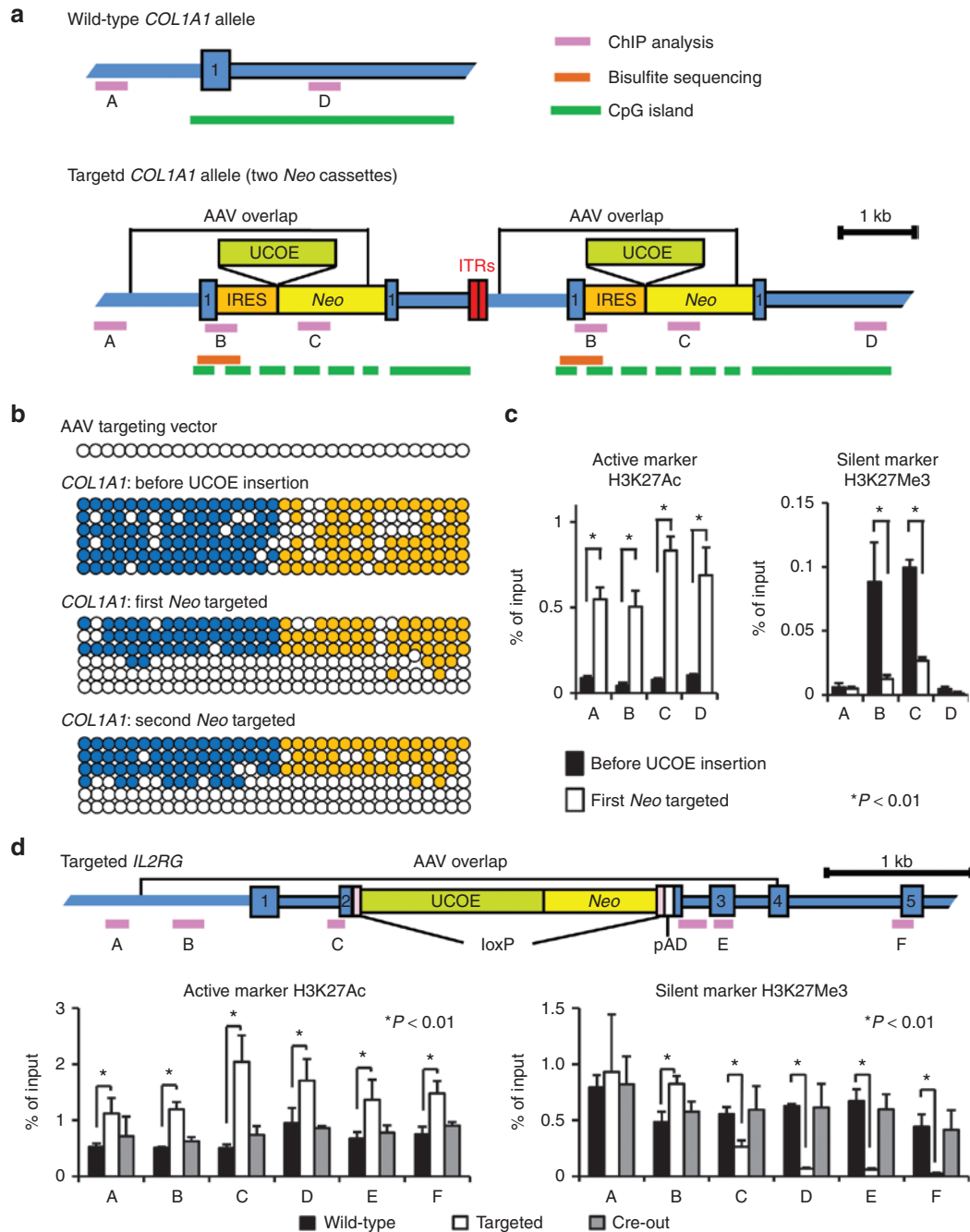


Figure 3 Epigenetic consequences of gene editing. **(a)** Structures of wild-type and IRES-*Neo* targeted *COL1A1* loci shown with rAAV overlap, UCOE insertion sites, and CpG islands. DNA fragments (A to D) amplified in ChIP assays and bisulfite sequencing regions are marked. **(b)** Methylation status of the region spanning from exon 1 of *COL1A1* (blue circles) to IRES (orange circles) in rAAV vector genomes, clone 1 genomic DNA, and clone 1 targeted at either the first or second *Neo* gene. Open and filled circles indicate unmethylated and methylated cytosines in CpGs, respectively. **(c)** The relative occupancies of H3K27Ac and H3K27Me3 in regions of the *COL1A1* locus before and after UCOE insertion as measured by ChIP analysis. **P* < 0.01. **(d)** Structure of the UCOE-*Neo* targeted *IL2RG* locus shown with rAAV overlap, loxP sites, and the locations of DNA fragments A to F amplified in ChIP assays. Histone occupancies were analyzed in age-matched wild-type, targeted, and Cre-out clones. **P* < 0.01.

both *IL2RG*-edited cultures (targeted and Cre-out; **Figure 4b**). The wild-type and umbilical cord blood cultures also expressed *IL2RG* (CD132) and supported the expansion of CD14⁻, CD56⁺ NK cells that could lyse MHC class I-negative target cells as expected, while the gene-edited cells did not (**Supplementary Figure S4a,b**), confirming that both the targeted and Cre-out alleles were functional knockouts. Importantly, the *IL2RG*-edited

lines were still able to produce monocytic and granulocytic CD14⁺ and CD15⁺ progeny (**Supplementary Figure S4c**). When EBs were cultured under T-cell differentiation conditions, the *IL2RG*-knockout cultures produced slightly fewer CD34⁺, CD7⁺ progenitors than wild-type cells at day 10, and these progenitors did not mature further and downregulate CD34 at later time points (**Figure 4c**). The *IL2RG*-knockout cells were capable

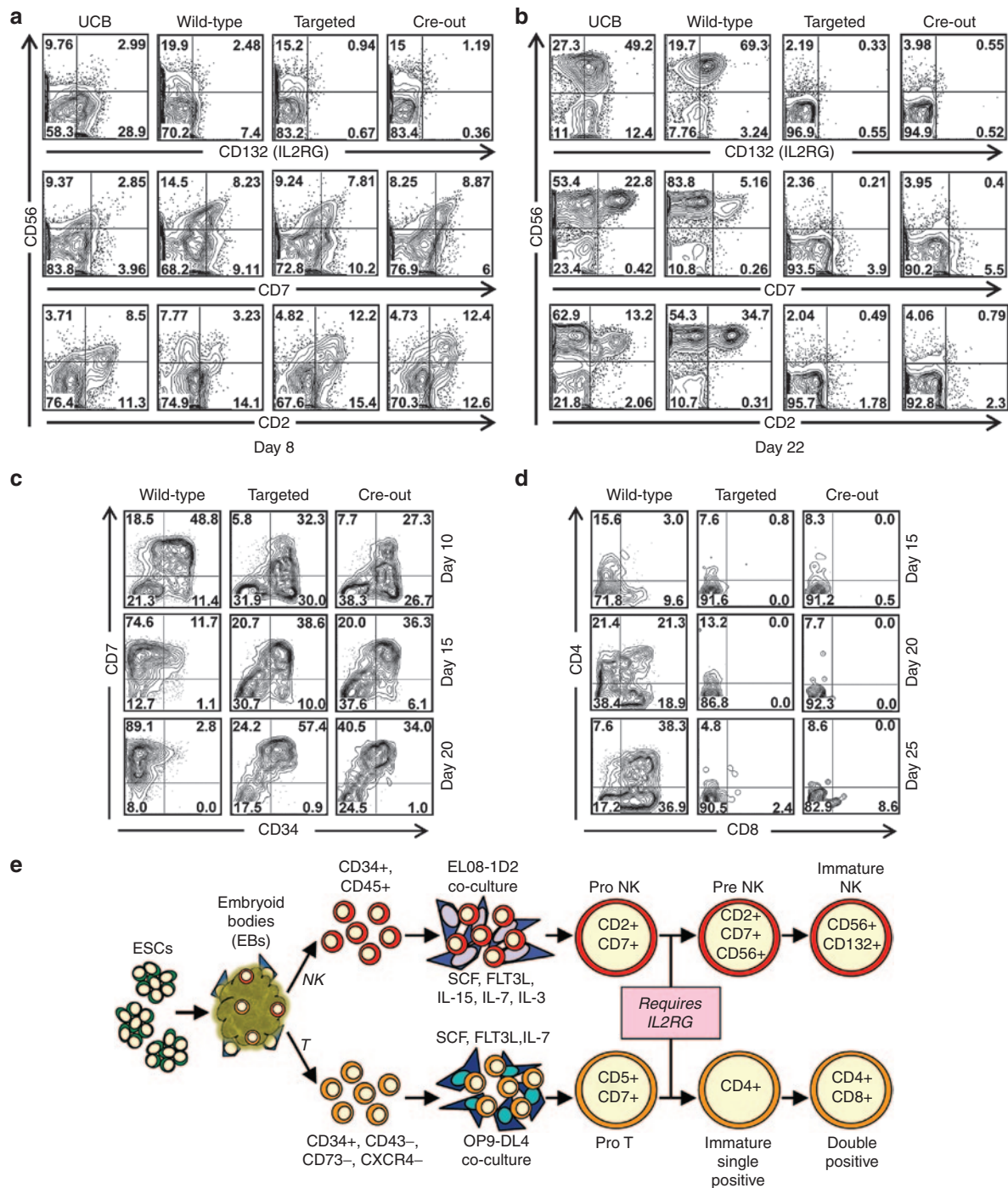


Figure 4 NK and T-cell differentiation of *IL2RG*-targeted human ESCs. **(a)** Flow cytometry analysis of CD2, CD7, CD132, and CD56 expression in day 8 NK cell differentiation cultures derived from UCB or wild-type, *IL2RG*-targeted or Cre-out ESC-derived EBs. **(b)** Same as **a** but assayed at 22 days. **(c)** Flow cytometry analysis of CD34 and CD7 expression T-cell differentiation cultures of wild-type, *IL2RG*-targeted or Cre-out ESCs harvested at the indicated day. **(d)** Same as **c** but analyzing CD4 and CD8 expression. **(e)** Working model of the differentiation block of *IL2RG*-knockout ESCs. EB, embryoid bodies; NK, natural killer; UCB, umbilical cord blood.

of producing CD5+, CD7+ pro-T cell progeny (**Supplementary Figure S4d**) but failed to produce more mature CD4+, CD8+, and double-positive (CD4+CD8+) T cells (**Figure 4d**). Both *IL2RG*-edited lines generated normal numbers of primitive and definitive erythroid/myeloid progenitors (data not shown). These combined data show that in a human ESC *in vitro* differentiation model, *IL2RG* expression is required for progression from

a CD7+ Pro-NK cell or Pro-T cell into more mature cell types (**Figure 4e**), confirming the well-known role of *IL2RG* in NK and T-cell development.

DISCUSSION

Here, we have described a robust method for editing silent loci in human PSCs without employing a nuclease. Our approach requires

the use of a UCOE promoter-driven selectable marker gene that resists silencing, rAAV vectors that efficiently deliver the targeting construct to PSCs, and subsequent selectable marker removal if desired. The UCOE promoter was superior to the other ubiquitously expressed promoters we tested, consistent with its known ability to maintain active chromatin.^{32–34} With this approach, 0.1–1% of the entire cell population undergoes gene editing, and these clones can be isolated by antibiotic selection. The *Neo* selection cassette used for *IL2RG* targeting could also function after random integration, and 1 out of 6 of G418-selected clones were accurately edited in those experiments, which is comparable to results obtained when using rAAV vectors to edit active human genes.³⁵ Cre-mediated recombination can be used to efficiently excise the transgene and produce a minimally altered locus that reverts to silent chromatin.

The raw (unselected) editing frequencies we obtained were similar to what has been reported for nuclease-based editing of silent genes in PSCs. For example, both our approach (**Supplementary Figure S2a**) and TALEN-based targeting of *IL2RG*⁶ led to gene editing in 0.14% of unselected PSCs. After antibiotic selection, 0.3–60% of PSC clones were edited by ZFN- or TALEN-based targeting of silent *PITX3* or *HBB* genes,^{3,5} which demonstrates the variability observed in these types of experiments, but still encompasses the 17% editing frequency we observed in G418-selected clones. An important advantage of our approach is that the rAAV vector does not include any nuclease or integrase proteins that might lead to unwanted on- or off-target mutations.^{6,8} And while rAAV can integrate randomly at spontaneously occurring chromosomal DSBs, infection with rAAV does not increase background mutation rates in cellular genes.³⁶ Random rAAV integrants are rarely found in edited PSC clones and can be easily ruled out by PCR or Southern blots for vector sequences.¹³ In contrast, the small in-del mutations produced by nonhomologous end joining at off-target, nuclease-induced DSBs can only be identified in an unbiased manner by full genome sequencing. This reduced genotoxicity of rAAV-mediated gene editing may be an advantage when preparing cells for clinical applications.

In settings where nuclease-induced genotoxicity can be tolerated or lowered to an acceptable level, our findings may also lead to further improvements in these gene-editing methods. Prior studies of silent gene editing in PSCs with ZFNs or TALENs used a PGK promoter to express the selectable marker,^{3–5} and our results suggest that using the UCOE promoter instead would have increased the number of edited clones that survived selection approximately fourfold (**Figure 1d**). Sequence-specific nucleases could also be combined with rAAV vectors for efficient delivery of both nuclease genes and UCOE-based targeting constructs to PSCs. Target-site DSBs can increase rAAV-mediated gene editing significantly,^{37,38} and rAAV-encoded ZFNs have been combined with rAAV targeting vectors for efficient *in vivo* gene editing,³⁹ demonstrating the potential of this approach. Finally, the recently developed Clustered, Regularly Interspaced Short Palindromic Repeat systems that employ guide RNAs to induce sequence-specific DSBs could also be combined with rAAV and provide further enhancements in silent gene editing, given the promising results obtained so far in CRISPR-based editing of expressed genes in human PSCs.^{40–42}

Our study begins to describe the epigenetic changes that can occur at an edited locus. We found that insertion of a UCOE promoter

into silent chromatin can lead to a loss of CpG island 5mC residues and convert histone modifications to a more active signature, but the details of these changes can be complex. For example, UCOE insertion increased H3K27Ac levels throughout the transcribed *Neo* cassette and into both upstream and downstream regions, but only reduced H3K27Me3 levels over a more localized region in the case of *COL1A1*, and only in downstream sequences in the case of *IL2RG*. The gene-editing process itself could have played a role in some of these changes, for example, by incorporating unmethylated vector DNA into the chromosome. Or alternatively, UCOE-dependent transcription could have indirectly altered the epigenetic signature, which may explain why some changes in histone modifications extended beyond the region of vector homology. Importantly, removal of the UCOE-*Neo* cassette caused the edited locus to return to an inactive epigenetic signature indistinguishable from the unedited, parental locus, based on the limited analysis we performed. However, a more detailed examination of the many other histone modifications that have been described,²⁶ as well as the identification of DNA-binding proteins,^{43,44} DNase hypersensitive sites,⁴⁵ and long-range chromatin interactions^{46,47} found at the locus, would presumably reveal additional epigenetic changes associated with gene editing, and it remains to be seen if all these changes convert back to a wild-type signature after removing the UCOE-*Neo* cassette.

Our choice of the *IL2RG* gene illustrates some of the potential applications of silent gene editing in PSCs. Edited PSCs can be used as cellular disease models to study the function of lineage-restricted genes. *IL2RG*-knockout PSCs were unable to differentiate into NK or T cells, confirming a central role for *IL2RG*-dependent signaling in the developing immune system²⁹ and demonstrating that the lack of NK and T cells observed in X-SCID patients^{27,28} is due to a differentiation block at the Pro T and Pro NK stage of lymphopoiesis. A similar rAAV editing strategy could be used to correct the *IL2RG* point mutations that typically cause X-SCID⁴⁸ so that patient-derived, gene-edited iPSCs could in principle be differentiated *ex vivo* into hematopoietic cells and transplanted into autologous recipients. *In vivo* selection should enrich for edited cells, and only a few cells would be required to correct the disease based on the mild phenotype of patients with spontaneous reversion mutations^{49,50} and the success of *IL2RG* gene therapy.⁵¹ TALEN-mediated gene editing was recently used to correct an *IL2RG* mutation in X-SCID iPSCs.⁷

IL2RG knockouts could also be used to prevent graft versus host disease when transplanting PSCs for therapeutic purposes, by eliminating PSC-derived T cells that may react against HLA-mismatched host cells. This would be especially valuable when using allogeneic PSC-derived cells to produce nonlymphoid hematopoietic cell types, such as macrophages and neutrophils to treat chronic granulomatous disease, or erythrocytes to treat hemoglobinopathies. In these settings, transplanted, PSC-derived hematopoietic stem/progenitor cells capable of long-term engraftment would continuously produce terminally differentiated therapeutic cell types in the absence of host-reactive allogeneic lymphoid cells. *IL2RG*-knockout cells may even be an advantage when transplanting autologous cells, because PSC-derived T and NK cells do not develop in a normal embryo and may not be educated appropriately to tolerate autologous host cells. Other scenarios can also be envisioned where preventing

the expression of a lineage-specification gene could produce a therapeutic advantage, such as PSCs with edited glucagon or somatostatin genes that can differentiate into insulin-secreting beta cells for the treatment of diabetes without producing the alpha or delta cells that frequently contaminate PSC-derived pancreatic islet cell preparations.^{52,53}

MATERIALS AND METHODS

Cell culture. H1 human ESCs⁵⁴ and human iPSC lines were cultured on mouse embryo fibroblasts as described.^{20,55} *COL1A1*-targeted G418-sensitive iPSCs were derived by reprogramming of (*COL1A1*-IRES-*Neo*)-targeted MSCs with lentiviral vectors as described.⁵⁵ 50 µg/ml active G418 was used for selection. Jurkat cells were cultured in RPMI-1640 with 10% FBS and 1% Pen/Strep (Life Technologies, Carlsbad, CA).

Viral vectors. AAV vector plasmids were assembled from PCR products by standard methods and confirmed by DNA sequencing. Homology arm fragments were amplified from the target cell type, and promoter fragments were amplified from H1 human ESCs and CF1 mice, respectively. The 1.2 kb UCOE fragment has been described and consists of nucleotides 26240199 to 26241411 of chromosome 7 (GRCh37/hg19).⁵⁶ Plasmid sequences are available upon request. AAV vectors were packaged in serotype 3b capsids by co-transfection of vector plasmids and packaging plasmid pDGM3B into 293T cells, purified by iodixanol step gradients, and their titers were determined by Southern blots as described.⁵⁷

Gene targeting. In promoter comparison experiments, 4×10^5 iPSCs were seeded in triplicate in 35-mm wells and transduced with rAAVs at a multiplicity of infection of 10^4 genome-containing particles/cell the next day. G418 selection was initiated 2 days after infection, and the surviving colonies were counted, picked, and expanded for further analysis. The total number of colony-forming units (CFU) was calculated by culturing 4×10^3 cells in a 6-cm dish without selection. In *IL2RG* targeting experiments, 5×10^5 wild-type H1 ESCs were seeded in a 10-cm dish and transduced with AAV at a multiplicity of infection of 3×10^3 genome-containing particles/cell the next day. Four days later, transduced ESCs were disaggregated into single cells using Accutase (Stemgent, Lexington, MA) and plated in serial dilutions in 10-cm dishes for G418 selection. 5×10^3 transduced H1 ESCs were also plated in a 10-cm dish without selection to determine the total number of CFUs. G418-resistant colonies were counted, picked, and screened initially by PCR to identify targeted clones.

Cre-mediated transgene removal. A polyclonal population of wild-type and *IL2RG*-targeted H1 ESCs was transduced as described with the nonintegrating foamy vector, N1FV-EokCreW, that expresses Cre recombinase.⁵⁵ Four days later, infected ESCs were disaggregated into single cells with Accutase, and serial dilutions were plated in 10-cm dishes. The surviving colonies were randomly picked and screened by PCR to identify age-matched clones with wild-type, UCOE-*Neo*-containing, or Cre-out *IL2RG* alleles for subsequent experiments.

DNA and RNA isolation. Genomic DNA was prepared from PSCs as described.^{57,58} Total cellular RNA was extracted by the Trizol method (Life Technologies) and used to generate cDNA with M-MLV reverse transcriptase and oligo-dT primers according to the manufacturer's protocol (Life Technologies).

Quantitative PCR and RT-PCR. cDNA qRT-PCR reactions were performed in triplicate with SYBR Select Master Mix (Life Technologies) on a StepOnePlus Real-Time PCR System (Life Technologies), and the relative gene expression levels were calculated by the $\Delta\Delta CT$ method. Homologous recombination frequencies were measured by infecting iPSCs with rAAV vectors, culturing for 5 days without selection, and determining the number of promoter-targeted alleles in 1 µg of genomic

DNA by Taqman qPCR (Life Technologies). Plasmids containing promoter-targeted *COL1A1* sequences were constructed by conventional cloning methods and used in qPCR reactions containing 0 to 10^4 plasmid molecules and 1 µg of wild-type genomic DNA (1.5×10^5 diploid genome equivalents) to generate standard curves.

Bisulfite sequencing. Genomic DNA was treated as described in the EZ DNA Methylation-Gold Kit (ZYMO Research, Irvine, CA) and used to PCR amplify *COL1A1* CpG island fragments. These PCR products were cloned into the pGEM-Teasy vector (Promega, Madison, WI), and the recombinant plasmids were sequenced.

Chromatin immunoprecipitation (ChIP). The ChIP protocol was adapted from Abcam's "X-ChIP protocol" (<http://www.abcam.com>) as follows. Three weeks after transduction with an AAV or Cre vector, PSCs with verified genotypes were dissociated with Accutase and fixed with PBS containing 1% formaldehyde at room temperature for 10 minutes with constant mixing. Fixation was stopped by adding glycine to a final concentration of 125 mmol/l. Samples were sonicated until chromatin was sheared to 500 to 1,000 bp. For binding, chromatin from 10^7 cells, 10 µg antibodies, and 30 µl solid protein-A/G beads (Santa Cruz Biotechnology, Dallas, TX) were combined and incubated at 4 °C overnight. After washing the beads, chromatin was eluted and incubated at 65 °C overnight to reverse cross-linking. The eluted chromatin was purified using a PCR purification kit (Qiagen, Valencia, CA) and used in qPCR reactions performed in triplicate with SYBR Select Master Mix (Life Technologies) on a StepOnePlus Real-Time PCR System (Life Technologies). Relative occupancy was calculated by the $\Delta\Delta CT$ method. Antibodies used were against H3K27me3 (Millipore, Billerica, MA), H3K27Ac (Abcam, Cambridge, MA), and normal rabbit IgG (Santa Cruz Biotechnology) as a control.

NK cell differentiation. NK differentiation was performed as described.^{30,59} Briefly, day 13 EBs were co-cultured with EL08-1D2 stromal cells in media supplemented with IL-3, IL7, IL-15, SCF, and FLT3L (Peprotech, Rocky Hill, NJ), and cells were harvested at appropriate time points for analysis. In chromium release assays, derived NK cells were stimulated by Clone 9.mbIL-21 aAPCs as described⁶⁰ and incubated with radioactive ⁵¹Cr-labeled K562 target cells, and lysis was measured by scintillation counter using the equation: % specific lysis = $100 \times (\text{test release} - \text{spontaneous release}) / (\text{maximal release} - \text{spontaneous release})$ as described.⁶¹ Flow cytometry was performed with a BD LSRII (BD Biosciences, Franklin Lakes, NJ) flow cytometer, and the data were analyzed by FlowJo software version 10.0 (Tree Star, Ashland, OR). Antibodies, which were used according to the manufacturers' recommendations, were from BD Biosciences unless otherwise indicated. Live cells were distinguished from dead cells by CYTOX blue dead cell stain (Life Technologies). Antibodies used for NK cell phenotype analysis were: CD56 (PE-Cy7-clone B159); CD7 (Alexa Fluor 700-clone M-T701); CD2 (PE-CF594-clone RPA-2.10); and CD132 (PE-clone TUGh4, eBioscience, San Diego, CA).

T-cell differentiation. T-cell differentiation and analysis were performed as described previously.³¹ Briefly, at day 8 of EB differentiation, 2×10^4 CD34+ CD43- CD73- CXCR4- cells isolated by fluorescence activated cell sorting were plated onto individual wells of a six-well plate containing OP9-DL4 stromal cells in the presence of rhFLT3L and rhIL-7. rhSCF was added for the first 7 days only (R&D Systems, Minneapolis, MN). Every 5 days, co-cultures were passaged onto fresh OP9-DL4 stromal cells. Cells were harvested and assayed at various time points. Cell suspensions were stained and analyzed on a BD LSR II flow cytometer. Data analysis was performed using FlowJo Software by gating on live cells followed by lack of DAPI uptake. Fluorophore-conjugated antibodies against CD4, CD5, CD7, CD8, CD34, and CD45 were purchased from BD Biosciences and eBioscience.

PCR Primers. All primer sequences are listed in **Supplementary Table S1**.

Statistical analysis. Statistical significance was assessed using the two-tailed Student's *t*-test. *P* values less than 0.01 were considered statistically significant. Data represent mean ± SEM of three.

SUPPLEMENTAL MATERIAL

Figure S1. Targeting a silent *COL1A1-IRES-Neo* cassette.

Figure S2. *IL2RG* targeting and UCOE-*Neo* removal.

Figure S3. CpG methylation at the *IL2RG* locus.

Figure S4. Characterization of T and NK cells derived from ESCs.

Table S1. Primer sequence.

ACKNOWLEDGMENTS

The authors thank Kristi Pilat, Roli Hirata, and Raisa Stolitenko for technical assistance and Els Henckaerts for helpful discussions. This work was supported by grants from the US NIH to D.W.R. (HL53750, DK55759), D.S.K. (Minnesota Partnership for Biotechnology), and G.K. (NIH U01HL100395 and CIHR MOP126117).

D.W.R. holds equity in Horizon Discovery and Universal Cells Inc. The other authors declare no competing financial interests.

REFERENCES

- Nickoloff, JA and Reynolds, RJ (1990). Transcription stimulates homologous recombination in mammalian cells. *Mol Cell Biol* **10**: 4837–4845.
- Thyagarajan, B, Johnson, BL and Campbell, C (1995). The effect of target site transcription on gene targeting in human cells *in vitro*. *Nucleic Acids Res* **23**: 2784–2790.
- Hockemeyer, D, Soldner, F, Beard, C, Gao, Q, Mitalipova, M, DeKaveler, RC *et al.* (2009). Efficient targeting of expressed and silent genes in human ESCs and iPSCs using zinc-finger nucleases. *Nat Biotechnol* **27**: 851–857.
- Zou, J, Mali, P, Huang, X, Dowey, SN and Cheng, L (2011). Site-specific gene correction of a point mutation in human iPSCs derived from an adult patient with sickle cell disease. *Blood* **118**: 4599–4608.
- Sun, N and Zhao, H (2014). Seamless correction of the sickle cell disease mutation of the HBB gene in human induced pluripotent stem cells using TALENs. *Biotechnol Bioeng* **111**: 1048–1053.
- Hendel, A, Kildebeck, EJ, Fine, EJ, Clark, JT, Punjia, N, Sebastiano, V *et al.* (2014). Quantifying genome-editing outcomes at endogenous loci with SMRT sequencing. *Cell Rep* **7**: 293–305.
- Menon, T, Firth, AL, Scripture-Adams, DD, Galic, Z, Qualls, SJ, Gilmore, WB *et al.* (2015). Lymphoid regeneration from gene-corrected SCID-X1 subject-derived iPSCs. *Cell Stem Cell* **16**: 367–372.
- Fu, Y, Foden, JA, Khayter, C, Maeder, ML, Reyon, D, Joung, JK *et al.* (2013). High-frequency off-target mutagenesis induced by CRISPR-Cas nucleases in human cells. *Nat Biotechnol* **31**: 822–826.
- Ripoche, MA, Kress, C, Poirier, F and Dandolo, L (1997). Deletion of the H19 transcription unit reveals the existence of a putative imprinting control element. *Genes Dev* **11**: 1596–1604.
- Tsai, TF, Bressler, J, Jiang, YH and Beaudet, AL (2003). Disruption of the genomic imprint in trans with homologous recombination at *Snrpn* in ES cells. *Genesis* **37**: 151–161.
- Lieberman-Lazarovich, M, Melamed-Bessudo, C, de Pater, S and Levy, AA (2013). Epigenetic alterations at genomic loci modified by gene targeting in *Arabidopsis thaliana*. *PLoS One* **8**: e85383.
- Russell, DW and Hirata, RK (1998). Human gene targeting by viral vectors. *Nat Genet* **18**: 325–330.
- Khan, IF, Hirata, RK, Wang, PR, Li, Y, Kho, J, Nelson, A *et al.* (2010). Engineering of human pluripotent stem cells by AAV-mediated gene targeting. *Mol Ther* **18**: 1192–1199.
- Li, LB, Chang, KH, Wang, PR, Hirata, RK, Papayannopoulou, T and Russell, DW (2012). Trisomy correction in Down syndrome induced pluripotent stem cells. *Cell Stem Cell* **11**: 615–619.
- Mitsui, K, Suzuki, K, Aizawa, E, Kawase, E, Suemori, H, Nakatsuiji, N *et al.* (2009). Gene targeting in human pluripotent stem cells with adeno-associated virus vectors. *Biochem Biophys Res Commun* **388**: 711–717.
- Chamberlain, JR, Schwarze, U, Wang, PR, Hirata, RK, Hankenson, KD, Pace, JM *et al.* (2004). Gene targeting in stem cells from individuals with osteogenesis imperfecta. *Science* **303**: 1198–1201.
- Wang, PR, Xu, M, Toffanin, S, Li, Y, Llovet, JM and Russell, DW (2012). Induction of hepatocellular carcinoma by *in vivo* gene targeting. *Proc Natl Acad Sci USA* **109**: 11264–11269.
- Rogers, CS, Hao, Y, Rokhlina, T, Samuel, M, Stoltz, DA, Li, Y *et al.* (2008). Production of CFTR-null and CFTR-DeltaF508 heterozygous pigs by adeno-associated virus-mediated gene targeting and somatic cell nuclear transfer. *J Clin Invest* **118**: 1571–1577.
- Sun, X, Yan, Z, Yi, Y, Li, Z, Lei, D, Rogers, CS *et al.* (2008). Adeno-associated virus-targeted disruption of the CFTR gene in cloned ferrets. *J Clin Invest* **118**: 1578–1583.
- Yu, J, Vodyanik, MA, Smuga-Otto, K, Antosiewicz-Bourget, J, Frane, JL, Tian, S *et al.* (2007). Induced pluripotent stem cell lines derived from human somatic cells. *Science* **318**: 1917–1920.
- Deyle, DR, Li, Y, Olson, EM and Russell, DW (2010). Nonintegrating foamy virus vectors. *J Virol* **84**: 9341–9349.
- Deaton, AM and Bird, A (2011). CpG islands and the regulation of transcription. *Genes Dev* **25**: 1010–1022.
- Deyle, DR, Li, LB, Ren, G and Russell, DW (2014). The effects of polymorphisms on human gene targeting. *Nucleic Acids Res* **42**: 3119–3124.
- Creyghton, MP, Cheng, AW, Welstead, GG, Kooistra, T, Carey, BW, Steine, EJ *et al.* (2010). Histone H3K27ac separates active from poised enhancers and predicts developmental state. *Proc Natl Acad Sci USA* **107**: 21931–21936.
- Rada-Iglesias, A, Bajpai, R, Swigut, T, Brugmann, SA, Flynn, RA and Wysocka, J (2011). A unique chromatin signature uncovers early developmental enhancers in humans. *Nature* **470**: 279–283.
- Ernst, J, Kheradpour, P, Mikkelsen, TS, Shores, N, Ward, LD, Epstein, CB *et al.* (2011). Mapping and analysis of chromatin state dynamics in nine human cell types. *Nature* **473**: 43–49.
- Noguchi, M, Yi, H, Rosenblatt, HM, Filipovich, AH, Adelstein, S, Modi, WS *et al.* (1993). Interleukin-2 receptor gamma chain mutation results in X-linked severe combined immunodeficiency in humans. *Cell* **73**: 147–157.
- Buckley, RH, Schiff, RI, Schiff, SE, Markert, ML, Williams, LW, Harville, TO *et al.* (1997). Human severe combined immunodeficiency: genetic, phenotypic, and functional diversity in one hundred eight infants. *J Pediatr* **130**: 378–387.
- Leonard, WJ (2001). Cytokines and immunodeficiency diseases. *Nat Rev Immunol* **1**: 200–208.
- Knorr, DA, Ni, Z, Hermanson, D, Hexum, MK, Bendzick, L, Cooper, LJ *et al.* (2013). Clinical-scale derivation of natural killer cells from human pluripotent stem cells for cancer therapy. *Stem Cells Transl Med* **2**: 274–283.
- Kennedy, M, Awong, G, Sturgeon, CM, Ditadi, A, LaMotte-Mohs, R, Zúñiga-Pflücker, JC *et al.* (2012). T lymphocyte potential marks the emergence of definitive hematopoietic progenitors in human pluripotent stem cell differentiation cultures. *Cell Rep* **2**: 1722–1735.
- Lindahl Allen, M and Antoniou, M (2007). Correlation of DNA methylation with histone modifications across the HNRPA2B1-CBX3 ubiquitously-acting chromatin open element (UCOE). *Epigenetics* **2**: 227–236.
- Müller-Kuller, U, Ackermann, M, Kolodziej, S, Brendel, C, Fritsch, J, Lachmann, N *et al.* (2015). A minimal ubiquitous chromatin opening element (UCOE) effectively prevents silencing of juxtaposed heterologous promoters by epigenetic remodeling in multipotent and pluripotent stem cells. *Nucleic Acids Res* **43**: 1577–1592.
- Pfaff, N, Lachmann, N, Ackermann, M, Kohlscheen, S, Brendel, C, Maetzig, T *et al.* (2013). A ubiquitous chromatin opening element prevents transgene silencing in pluripotent stem cells and their differentiated progeny. *Stem Cells* **31**: 488–499.
- Hirata, R, Chamberlain, J, Dong, R and Russell, DW (2002). Targeted transgene insertion into human chromosomes by adeno-associated virus vectors. *Nat Biotechnol* **20**: 735–738.
- Miller, DG, Petek, LM and Russell, DW (2004). Adeno-associated virus vectors integrate at chromosome breakage sites. *Nat Genet* **36**: 767–773.
- Porteus, MH, Cathomen, T, Weitzman, MD and Baltimore, D (2003). Efficient gene targeting mediated by adeno-associated virus and DNA double-strand breaks. *Mol Cell Biol* **23**: 3558–3565.
- Miller, DG, Petek, LM and Russell, DW (2003). Human gene targeting by adeno-associated virus vectors is enhanced by DNA double-strand breaks. *Mol Cell Biol* **23**: 3550–3557.
- Li, H, Haurigot, V, Doyon, Y, Li, T, Wong, SY, Bhagwat, AS *et al.* (2011). *In vivo* genome editing restores haemostasis in a mouse model of haemophilia. *Nature* **475**: 217–221.
- Mali, P, Yang, L, Esvelt, KM, Aach, J, Guell, M, DiCarlo, JE *et al.* (2013). RNA-guided human genome engineering via Cas9. *Science* **339**: 823–826.
- Hou, Z, Zhang, Y, Propson, NE, Howden, SE, Chu, LF, Sontheimer, EJ *et al.* (2013). Efficient genome engineering in human pluripotent stem cells using Cas9 from *Neisseria meningitidis*. *Proc Natl Acad Sci USA* **110**: 15644–15649.
- Ding, Q, Regan, SN, Xia, Y, Oostrom, LA, Cowan, CA and Musunuru, K (2013). Enhanced efficiency of human pluripotent stem cell genome editing through replacing TALENs with CRISPRs. *Cell Stem Cell* **12**: 393–394.
- The ENCODE Project Consortium. (2012). An integrated encyclopedia of DNA elements in the human genome. *Nature* **489**: 57–74.
- Kharchenko, PV, Tolstorukov, MY and Park, PJ (2008). Design and analysis of ChIP-seq experiments for DNA-binding proteins. *Nat Biotechnol* **26**: 1351–1359.
- Thurman, RE, Rynes, E, Humbert, R, Vierstra, J, Maurano, MT, Haugen, E *et al.* (2012). The accessible chromatin landscape of the human genome. *Nature* **489**: 75–82.
- Sanyal, A, Lajoie, BR, Jain, G and Dekker, J (2012). The long-range interaction landscape of gene promoters. *Nature* **489**: 109–113.
- de Wit, E, Bouwman, BA, Zhu, Y, Klous, P, Splinter, E, Verstegen, MJ *et al.* (2013). The pluripotent genome in three dimensions is shaped around pluripotency factors. *Nature* **501**: 227–231.
- Puck, JM, Pepper, AE, Henthorn, PS, Candotti, F, Isakov, J, Whitwam, T *et al.* (1997). Mutation analysis of *IL2RG* in human X-linked severe combined immunodeficiency. *Blood* **89**: 1968–1977.
- Kuijpers, TW, van Leeuwen, EM, Barendregt, BH, Klarenbeek, P, aan de Kerk, DJ, Baars, PA *et al.* (2013). A reversion of an *IL2RG* mutation in combined immunodeficiency providing competitive advantage to the majority of CD8+ T cells. *Haematologica* **98**: 1030–1038.
- Speckmann, C, Pannicke, U, Wiech, E, Schwarz, K, Fisch, P, Friedrich, W *et al.* (2008). Clinical and immunologic consequences of a somatic reversion in a patient with X-linked severe combined immunodeficiency. *Blood* **112**: 4090–4097.
- Cavazzana-Calvo, M, Hacein-Bey, S, de Saint Basile, G, Gross, F, Yvon, E, Nusbaum, P *et al.* (2000). Gene therapy of human severe combined immunodeficiency (SCID)-X1 disease. *Science* **288**: 669–672.
- D'Amour, KA, Bang, AG, Eliazar, S, Kelly, OG, Agulnick, AD, Smart, NG *et al.* (2006). Production of pancreatic hormone-expressing endocrine cells from human embryonic stem cells. *Nat Biotechnol* **24**: 1392–1401.
- Jiang, J, Au, M, Lu, K, Eshpeter, A, Korbitt, G, Fisk, G *et al.* (2007). Generation of insulin-producing islet-like clusters from human embryonic stem cells. *Stem Cells* **25**: 1940–1953.

54. Thomson, JA, Itskovitz-Eldor, J, Shapiro, SS, Waknitz, MA, Swiergiel, JJ, Marshall, VS *et al.* (1998). Embryonic stem cell lines derived from human blastocysts. *Science* **282**: 1145–1147.
55. Deyle, DR, Khan, IF, Ren, G, Wang, PR, Kho, J, Schwarze, U *et al.* (2012). Normal collagen and bone production by gene-targeted human osteogenesis imperfecta iPSCs. *Mol Ther* **20**: 204–213.
56. Zhang, F, Frost, AR, Blundell, MP, Bales, O, Antoniou, MN and Thrasher, AJ (2010). A ubiquitous chromatin opening element (UCOE) confers resistance to DNA methylation-mediated silencing of lentiviral vectors. *Mol Ther* **18**: 1640–1649.
57. Khan, IF, Hirata, RK and Russell, DW (2011). AAV-mediated gene targeting methods for human cells. *Nat Protoc* **6**: 482–501.
58. Papapetrou, EP and Sadelain, M (2011). Derivation of genetically modified human pluripotent stem cells with integrated transgenes at unique mapped genomic sites. *Nat Protoc* **6**: 1274–1289.
59. McCullar, V, Oostendorp, R, Panoskaltis-Mortari, A, Yun, G, Lutz, CT, Wagner, JE *et al.* (2008). Mouse fetal and embryonic liver cells differentiate human umbilical cord blood progenitors into CD56-negative natural killer cell precursors in the absence of interleukin-15. *Exp Hematol* **36**: 598–608.
60. Denman, CJ, Senyukov, VV, Somanchi, SS, Phatarpekar, PV, Kopp, LM, Johnson, JL *et al.* (2012). Membrane-bound IL-21 promotes sustained ex vivo proliferation of human natural killer cells. *PLoS One* **7**: e30264.
61. Miller, JS, Oelkers, S, Verfaillie, C and McClave, P (1992). Role of monocytes in the expansion of human activated natural killer cells. *Blood* **80**: 2221–2229.